American College of Rheumatology
Empowering Rheumatology Professionals

Arthritis & Rheumatology
Vol. 74, No. 6, June 2022, pp 1070–1082
DOI 10.1002/art.42052

Contribution of Interleukin-4–Induced Epithelial Cell Senescence to Glandular Fibrosis in IgG4-Related Sialadenitis

Sai-Nan Min,[1] Meng-Qi Zhu,[1] Xiang-Di Mao,[2] Wei Li,[1] Tai Wei,[1] Mei Mei,[1] Yan Zhang,[2] Li-Ling Wu,[2] Guang-Yan Yu,[1] and Xin Cong[2]

Objective. IgG4-related sialadenitis (IgG4-RS) is a chronic fibroinflammatory disease characterized by glandular fibrosis and hyposalivation. This study was undertaken to explore the role of cellular senescence in the pathogenesis of IgG4-RS–related fibrosis.

Methods. The expression of senescence markers and proinflammatory cytokines in the submandibular glands (SMGs) of IgG4-RS patients (n = 18) and controls (n = 14) was determined by proteomics, real-time polymerase chain reaction, Western blotting, and immunohistochemistry. After interleukin-4 (IL-4) treatment, high-throughput RNA sequencing was performed to identify the differentially expressed genes in SMG-C6 cells. A glandular fibrosis model was established by the intraglandular injection of IL-4 into mouse SMGs (n = 8 per group).

Results. Salivary acinar and ductal epithelial cells underwent senescence in IgG4-RS patients, as indicated by the elevated activity of senescence-associated β-galactosidase, lipofuscin accumulation, enhanced expression of senescence markers (p53 and $p16^{INK4A}$), and up-regulation of senescence-associated secretory phenotype factors. Moreover, there was a significant increase in IL-4 levels in SMGs from IgG4-RS patients ($P < 0.01$), which positively correlated with $p16^{INK4A}$ expression and the fibrosis score. Incubation with IL-4 exacerbated salivary epithelial cell senescence by increasing the expression of $p16^{INK4A}$ through the reactive oxygen species (ROS)/p38 MAPK pathway. Supernatant collected from IL-4–induced senescent SMG-C6 cells enhanced fibroblast activation and matrix protein production ($P < 0.05$). Furthermore, injecting mice with IL-4 promoted fibrosis and senescence phenotypes in SMGs in vivo.

Conclusion. The cellular senescence induced by IL-4 through the ROS/p38 MAPK-$p16^{INK4A}$ pathway promotes fibrogenesis in IgG4-RS. Our data suggest that cellular senescence could serve as a novel therapeutic target for treating IgG4-RS.

INTRODUCTION

IgG4-related disease (IgG4-RD) is a systemic fibroinflammatory disorder characterized by increased IgG4+ plasma cell infiltration and storiform fibrosis in multiple organs, such as the salivary glands, pancreas, lacrimal glands, and kidney (1). Salivary glands were found to be affected in nearly 27–58% of IgG4-RD patients, and this condition is referred to as "IgG4-related sialadenitis (IgG4-RS)" (2–4). IgG4-RS patients exhibit persistent and painless unilateral or bilateral enlargement of the salivary glands,

Supported by the National Natural Science Foundation of China (grants 81671005, 81974151, 81771093, 81991500, 81991502, and 82101037).

[1]Sai-Nan Min, PhD, Meng-Qi Zhu, MSc, Wei Li, MD, Tai Wei, PhD, Mei Mei, PhD, Guang-Yan Yu, DDS, PhD: Peking University School and Hospital of Stomatology, National Center of Stomatology, National Clinical Research Center for Oral Diseases, National Engineering Research Center of Oral Biomaterials and Digital Medical Devices, Beijing Key Laboratory of Digital Stomatology, Research Center of Engineering and Technology for Computerized Dentistry Ministry of Health, and NMPA Key Laboratory for Dental Materials, Beijing, China; [2]Xiang-Di Mao, BS, Yan Zhang, PhD, Li-Ling Wu, MSc, Xin Cong, PhD: Peking University School of Basic Medical Sciences, Key Laboratory of Molecular Cardiovascular Sciences, Ministry of Education, and Beijing Key Laboratory of Cardiovascular Receptors Research, Beijing, China.

Drs. Yu and Cong contributed equally to this work.

Author disclosures are available at https://onlinelibrary.wiley.com/action/downloadSupplement?doi=10.1002%2Fart.42052&file=art42052-sup-0001-Disclosureform.pdf.

Address correspondence to Guang-Yan Yu, DDS, PhD, Department of Oral and Maxillofacial Surgery, Peking University School and Hospital of Stomatology, No. 22, Zhongguancun South Avenue, Haidian District, Beijing 100081, China (email: gyyu@263.net); or to Xin Cong, PhD, Department of Physiology and Pathophysiology, Peking University School of Basic Medical Sciences, No. 38, Xueyuan Road, Haidian District, Beijing 100191, China (email: congxin@bjmu.edu.cn).

Submitted for publication August 24, 2021; accepted in revised form December 14, 2021.

which is accompanied by different degrees of hyposecretion due to progressive fibrosis (5).

In a cohort of 235 consecutive IgG4-RD patients in Japan, nine-tenths of the cases were diagnosed in 50–70-year-old individuals, suggesting that IgG4-RD mainly occurs in middle-aged and elderly individuals (6). The onset of this disease was more likely to be associated with strong lymphocytic activation in elderly patients (ages >70 years) than in younger patients (7). Recent studies have shown that serum interleukin-15 (IL-15) levels are increased in IgG4-RS patients. Furthermore, the number of memory CD28–CD4+ T cells, which proliferate in response to IL-15, also increased with age (8–10). Given that many chronic inflammatory diseases are considered to be aging-related disorders, it is notable that some features associated with aging, such as interstitial fibrosis, acinar atrophy, persistent inflammation, and loss of regenerative capability in salivary gland epithelial cells, are observed in IgG4-RS (5). These findings suggest that aging might be a contributing factor to the initiation and progression of IgG4-RS.

Accumulation of cellular senescence is a main feature of aged organisms, and refers to a state of irreversible growth arrest, which is triggered by pathogenic factors, such as inflammation caused by diverse inflammatory cytokines (e.g., interleukins, interferons, and chemokines), oxidative stress, oncogene activation, and DNA damage (11,12). The characteristics of senescent cells include growth arrest, increased lysosomal content, resistance to apoptosis, an enlarged and flattened morphology, and enhanced expression of cyclin-dependent kinase (CDK) inhibitor genes, such as $p16^{INK4A}$, p21, and p15 (13). Accumulation of senescent cells can further promote the release of proinflammatory cytokines, chemokines, growth factors, and proteases that are known as senescence-associated secretory phenotype (SASP) factors. SASP factors secreted by senescent cells reinforce and propagate senescence in an autocrine and paracrine manner; in addition, they attract immune cells and promote tissue repair (14).

Several studies have indicated that many proinflammatory cytokines, such as IL-18, transforming growth factor β (TGFβ), and IL-22, can induce cellular senescence and participate in various fibrotic diseases, such as idiopathic pulmonary fibrosis, liver fibrosis, and kidney fibrosis (15–17). Furthermore, cellular senescence has been observed and is related to the loss of salivary gland function in mice that received radiation in the head and neck, in primary Sjögren's syndrome, and in the senescence-accelerated mouse prone 1 line (18–22). However, whether the infiltrating lymphocytes and their secreted proinflammatory cytokines trigger cellular senescence in the salivary glands of patients with IgG4-RS remains unexplored. In this study, we aimed to understand the presence and role of cellular senescence in the pathogenesis of fibrosis in the salivary glands of patients with IgG4-RS, and further elucidate the underlying mechanism.

MATERIALS AND METHODS

Cell culture, animal models, Sudan Black B staining, senescence-associated (SA) β-galactosidase (β-gal) staining, TUNEL staining, Masson's trichrome staining, sirius red staining, lactate dehydrogenase (LDH) assay, cell cycle and proliferation assays, 5-ethynyl-2′-deoxyuridine assay, measurement of reactive oxygen species (ROS), migration assay, proteomics analysis, RNA sequencing, cytokine array, etc. are described in detail in the Supplementary Methods, available on the *Arthritis & Rheumatology* website at http://onlinelibrary.wiley.com/doi/10.1002/art.42052. All animal research has been reported according to Animals in Research: Reporting In Vivo Experiments guidelines (23).

Patients and samples. Submandibular gland (SMG) biopsy specimens were obtained from 18 patients who were diagnosed as having IgG4-RS according to the comprehensive diagnostic criteria (24) and had not been treated with steroids or immunosuppressants. SMG tissues from 4 patients with chronic sialadenitis (mean ± SD age 57.00 ± 8.29 years) were included for comparison. Control SMG tissues, confirmed to be normal on pathologic examination, were obtained from 14 individuals (mean ± SD age 62.50 ± 6.37 years) undergoing surgery for head or neck carcinoma. Immediately after surgery, a part of the specimen was frozen in liquid nitrogen for RNA and protein extraction, and the remainder was used for histochemical staining. Blood samples were obtained from IgG4-RS patients and healthy donors after an overnight fast. Following sample collection, serum was immediately separated by centrifugation and stored at −80°C. All patients signed an informed consent form. The study protocol was approved by the Ethics Committee of Peking University School and Hospital of Stomatology (No. PKUSSORB-2013008). The clinical characteristics and serologic features of the IgG4-RS patients are summarized in Supplementary Table 1, available on the *Arthritis & Rheumatology* website at http://onlinelibrary.wiley.com/doi/10.1002/art.42052.

Statistical analysis. Data were normalized and are expressed as the mean ± SEM. The significance of differences between groups was analyzed by Student's unpaired *t*-test or analysis of variance followed by Bonferroni test or Tukey's test using GraphPad software. Correlation was analyzed by Pearson's correlation coefficient analysis. *P* values less than 0.05 were considered significant.

RESULTS

Altered expression profile of aging-related proteins in the SMGs of patients with IgG4-RS. The protein profiles of SMG samples from IgG4-RS patients and controls were screened using proteomics. A total of 894 differentially expressed

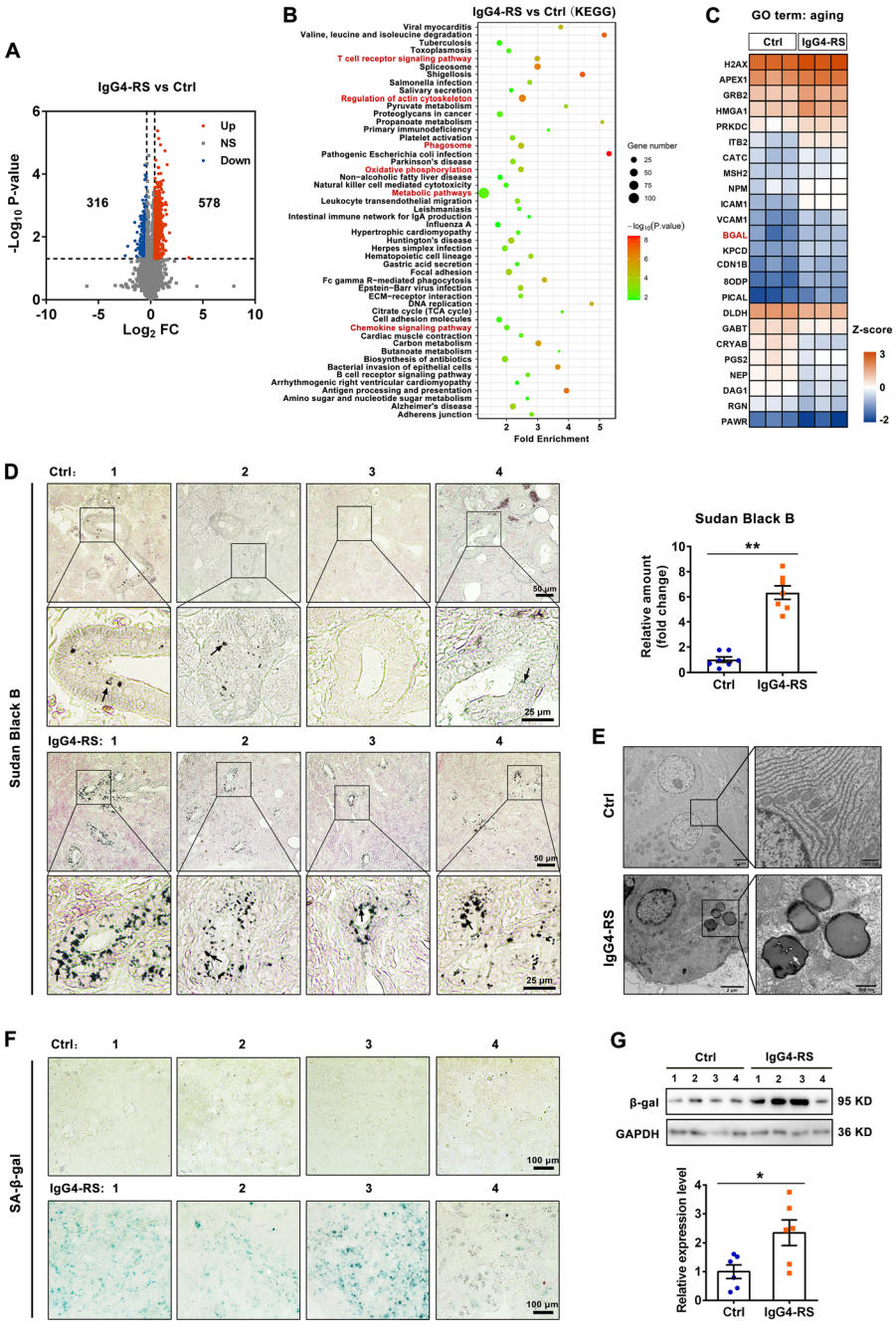

Figure 1. Cellular senescence in the submandibular glands (SMGs) of patients with IgG4-related sialadenitis (IgG4-RS). **A**, Volcano plot displaying differential expression of 894 proteins in IgG4-RS patients and controls (n = 3 per group). Proteins up-regulated (ratio of fold change [FC] ≥1.3) in IgG4-RS are shown in orange; proteins down-regulated (ratio of fold change ≤0.77) in IgG-RS are shown in blue. NS = not significant. **B**, The 50 most enriched KEGG pathways for the differentially expressed proteins in SMGs from IgG4-RS patients and controls. Pathways shown in red are related to aging and inflammatory processes. ECM = extracellular matrix; TCA = tricarboxylic acid. **C**, Heatmap depicting differentially expressed proteins in the Gene Ontology term "aging" in controls and IgG4-RS patients. Several aging-related proteins, such as β-galactosidase (β-gal), histone H2AX, and CDK inhibitor 1B were abnormally expressed in SMGs from IgG4-RS patients. Red text indicates β-gal, a cellular senescence marker. **D**, Left, Sudan Black B staining for lipofuscins in SMGs from 4 representative controls (n = 7) and 4 representative IgG4-RS patients (n = 7). Bottom panels show higher-magnification views (bars = 25 μm) of the boxed areas in the top panels (bars = 50 μm). **Arrows** indicate positive staining. Right, Quantitative analysis of Sudan Black B staining. Symbols represent individual subjects; bars show the mean ± SEM. **E**, Representative transmission electron microscopy images showing an accumulation of lipofuscins in the SMG from an IgG4-RS patient. Right panels (bars = 500 nm) show higher-magnification views of the boxed areas in the left panels (bars = 2 μm). **F**, Senescence-associated (SA) β-gal staining in SMGs from controls and IgG4-RS patients (n = 4 per group). Bars = 100 μm. **G**, Western blot (top) and quantification (bottom) of β-gal expression in SMGs from controls and IgG4-RS patients (n = 6 per group). Symbols represent individual subjects; bars show the mean ± SEM. * = $P < 0.05$; ** = $P < 0.01$.

proteins were identified (ratio of fold change ≥1.3 or ≤0.77; $P < 0.05$), of which 578 were up-regulated and 316 were down-regulated in IgG4-RS (Figure 1A). KEGG pathway enrichment analysis revealed that the differentially expressed proteins were enriched in 84 pathways. The top 50 pathways followed a pattern similar to the aging process and included metabolic pathways, oxidative phosphorylation, and regulation of actin cytoskeleton, as well as pathways related to inflammatory processes (Figure 1B). Accordingly, we further analyzed the term "Aging" in Gene Ontology (GO)–enriched categories. Several aging-related proteins, such as β-gal, histone H2AX, and CDK inhibitor 1B were abnormally expressed in the SMGs of IgG4-RS patients (Figure 1C). These results implied that aging might be involved in the pathogenesis of IgG4-RS.

Epithelial cell senescence in the SMGs of patients with IgG4-RS. Sudan Black B and SA β-gal staining are 2 frequently used methods to evaluate cellular senescence. SA β-gal staining measures the activity of the lysosomal enzyme β-gal, a well-known marker of cellular senescence, whereas Sudan Black B staining directly detects the cellular aging process via the waste product lipofuscin, a hallmark of senescent cells (25,26). We observed more Sudan Black B–stained granules in the ductal cells in SMGs from IgG4-RS patients than in those from controls (Figure 1D). The accumulation of lipofuscins in the ductal cells in SMGs from IgG4-RS patients was further confirmed using electron microscopy (Figure 1E). SA β-gal staining indicated a significant increase in SA β-gal activity in SMGs from IgG4-RS patients compared with those from controls (Figure 1F). The increased β-gal protein expression was further validated by Western blotting (Figure 1G).

The expression of multiple senescence markers, such as $p14^{ARF}$, p53, and $p16^{INK4A}$, and SASP factors, such as IL-6 and TGFβ1, was higher in SMGs from IgG4-RS patients than in those from controls. In contrast, the levels of messenger RNA (mRNA) for p21 were unchanged (Figure 2A). The p53 and $p16^{INK4A}$ protein levels were significantly elevated in SMGs from IgG4-RS patients; however, only a slight, although significant, increase in the expression of p21 protein was detected (Figure 2B). Furthermore, increased intensities of p53 and $p16^{INK4A}$ were seen in the residual acinar and ductal cells of SMGs from IgG4-RS patients. Additionally, sporadic expression of p21 was observed (Figure 2C).

Since p21 signal was not activated, we did not further examine the expression and localization of its upstream molecule $p14^{ARF}$. However, there was no significant increase in lipofuscin or $p16^{INK4A}$ expression in SMGs from patients with chronic sialadenitis, a nonspecific inflammatory and fibrotic disease (Supplementary Figures 1A and B, available on the *Arthritis & Rheumatology* website at http://onlinelibrary.wiley.com/doi/10.1002/art.42052), indicating that cellular senescence might be specific to IgG4-RS. Both the proportion of apoptotic cells and the expression of cleaved caspase 3 were unchanged among IgG4-RS patients and controls (Supplementary Figures 2A and B, available on the *Arthritis & Rheumatology* website at http://onlinelibrary.wiley.com/doi/10.1002/art.42052), suggesting that apoptosis might not be the major pathologic process in IgG4-RS. These results indicate that both acinar and ductal epithelial cells undergo cellular senescence in IgG4-RS.

Elevated IL-4 expression in the SMGs of patients with IgG4-RS. The infiltration of lymphocytes plays a crucial role in the progression of IgG4-RS (27,28). CD20+ B cells were primarily located within the germinal centers, whereas CD3+ T lymphocytes were organized around germinal centers. Among CD3+ T lymphocytes, CD4+ T cells were the dominant population in SMGs from IgG4-RS patients (Figure 2D). The levels of CD4+ T cell–associated cytokines, such as IL-2, interferon-γ (IFNγ), IL-4, IL-13, and IL-10, were significantly higher in IgG4-RS patients than in controls. IL-4 in particular was one of the proinflammatory cytokines that was most up-regulated (Figure 2E). The increase in IL-4 protein expression, together with the increase in IL-4 receptor (IL-4R) mRNA, in SMGs from IgG4-RS patients was further validated by Western blotting and real-time polymerase chain reaction, respectively (Figures 2F and G).

We then costained SMGs with IL-4 and zonula occludens 1, a tight junction molecule expressed in epithelial cells. Expression of IL-4 was not found in controls and was slightly detected in SMGs from patients with chronic sialadenitis (Supplementary Figure 3A, available on the *Arthritis & Rheumatology* website at http://onlinelibrary.wiley.com/doi/10.1002/art.42052). In contrast, strong IL-4 staining was detectable in the inflammatory infiltration foci of SMGs from IgG4-RS patients (Figure 2H). Notably, IL-4 was partially colocalized with or accumulated surrounding CD4+ lymphocytes in SMGs from IgG4-RS patients, whereas IL-4 and CD4 staining was hardly observed in controls (Supplementary Figure 3B, available on the *Arthritis & Rheumatology* website at http://onlinelibrary.wiley.com/doi/10.1002/art.42052), indicating that a portion of IL-4 was produced or secreted from Th2 cells. Furthermore, a cytokine antibody array was performed to determine the cytokine profiles in the serum of IgG4-RS patients and controls. The levels of multiple cytokines, such as granulocyte-macrophage colony stimulating factor, IL-23, TGFβ, and tumor necrosis factor α, were higher among IgG4-RS patients (Supplementary Figure 4, available on the *Arthritis & Rheumatology* website at http://onlinelibrary.wiley.com/doi/10.1002/art.42052). In contrast, serum IL-4 levels were unchanged, suggesting that local IL-4 might play an important role in IgG4-RS.

To further study the relationship between IL-4 and cellular senescence, correlation analysis was performed. IL-4 mRNA expression positively correlated with the senescence marker $p16^{INK4A}$, but not with p53 or p21, in SMGs from IgG4-RS patients (Figure 2I). These results suggest that an association

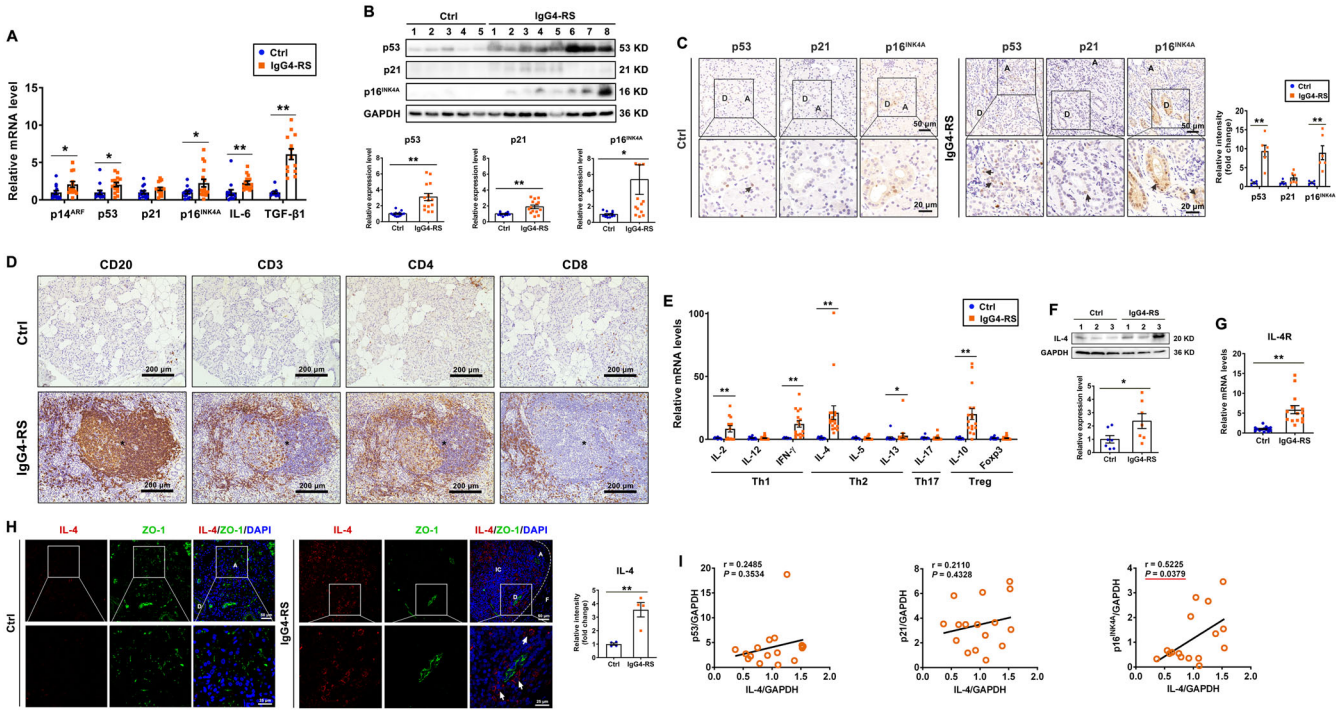

Figure 2. Relationship between elevated interleukin-4 (IL-4) expression and senescence in submandibular glands (SMGs) from patients with IgG4-related sialadenitis (IgG4-RS). **A**, Expression of mRNA for $p14^{ARF}$, p53, p21, $p16^{INK4A}$, IL-6, and transforming growth factor β1 (TGFβ1) in SMGs from controls (n = 11–14) and IgG4-RS patients (n = 13–16). **B**, Western blot (top) and quantification (bottom) of p53, p21, and $p16^{INK4A}$ protein expression in SMGs from controls (n = 12) and IgG4-RS patients (n = 14). **C**, Left, Immunostaining for p53, p21, and $p16^{INK4A}$ in SMGs from a control and an IgG4-RS patient. Bottom panels (bars = 20 μm) show higher-magnification views of the boxed areas in the top panels (bars = 50 μm). **Arrows** indicate positive staining. Right, Relative staining intensity in SMGs from controls (n = 5) and IgG4-RS patients (n = 6). **D**, Immunostaining for CD20, CD3, CD4, and CD8 in SMGs from a control and an IgG4-RS patient. **Asterisks** indicate lymphoid follicles. Bars = 200 μm. **E**, Levels of mRNA for IL-2, IL-12, interferon-γ (IFNγ), IL-4, IL-5, IL-13, IL-17, IL-10, and FoxP3 in SMGs from controls (n = 8–14) and IgG4-RS patients (n = 12–18). **F**, Western blot (top) and quantification (bottom) of IL-4 protein levels in SMGs from controls and IgG4-RS patients (n = 7 per group). **G**, Levels of mRNA for IL-4 receptor (IL-4R) in SMGs from controls and IgG4-RS patients (n = 14 per group). **H**, Left, Immunostaining for IL-4 and zonula occludens 1 (ZO-1) in SMGs from a control and an IgG4-RS patient. Bottom panels (bars = 25 μm) show higher-magnification views of the boxed areas in the top panels (bars = 50 μm). Right, Relative staining intensity in SMGs from controls and IgG4-RS patients (n = 4 per group). **I**, Correlations between the levels of IL-4 mRNA and senescence markers in SMGs from IgG4-RS patients (n = 16), determined by Spearman's test. In **A**–**C** and **E**–**H**, symbols represent individual subjects; bars show the mean ± SEM. * = $P < 0.05$; ** = $P < 0.01$. **A** = acini; **D** = ductal cells; **IC** = inflammatory cells; **F** = fibrosis. Color figure can be viewed in the online issue, which is available at http://onlinelibrary.wiley.com/doi/10.1002/art.42052/abstract.

exists between augmented IL-4 and cellular senescence in SMG lesions in IgG4-RS patients.

IL-4–induced cellular senescence in SMG-C6 cells. Considering that there is not a commonly accepted salivary gland ductal cell line, we chose to use SMG-C6 cells, a rat submandibular epithelial cell line with characteristics of acinar cells, for the in vitro studies. First, high-throughput RNA sequencing was performed in SMG-C6 cells with or without recombinant IL-4 stimulation. A total of 654 genes with significant differential expression were identified (ratios of fold change ≥2 or ≤0.5; $P < 0.05$), of which 434 were up-regulated and 220 were down-regulated (Figure 3A). The 20 most enriched biologic processes for significantly down-regulated and up-regulated genes are shown in Figure 3B and Supplementary Figure 5, available on the *Arthritis & Rheumatology* website at http://onlinelibrary.wiley.com/doi/10.1002/art.42052, respectively. Notably, the down-regulated genes related to the regulation of cell proliferation were screened, while the up-regulated genes were enriched in positive regulation of cell migration and localization.

Since low proliferation is one of the characteristics of senescent cells, we speculated that IL-4 could induce salivary gland cell senescence. Treating SMG-C6 cells with IL-4 for 48 hours led to inhibition of the proliferative capacity (Figures 3C and D). Cells exposed to IL-4 were arrested in the S phase (Figure 3E). Furthermore, IL-4 treatment significantly increased the activity of SA β-gal and caused a flattening and enlargement of cell morphology (Figure 3F). However, IL-4 neutralizing antibody significantly eliminated the IL-4–induced increase in SA β-gal activity and growth inhibition (Supplementary Figures 6A and B, available on the *Arthritis & Rheumatology* website at http://onlinelibrary.wiley.com/doi/10.1002/art.42052), again suggesting a direct relationship between IL-4 and senescence.

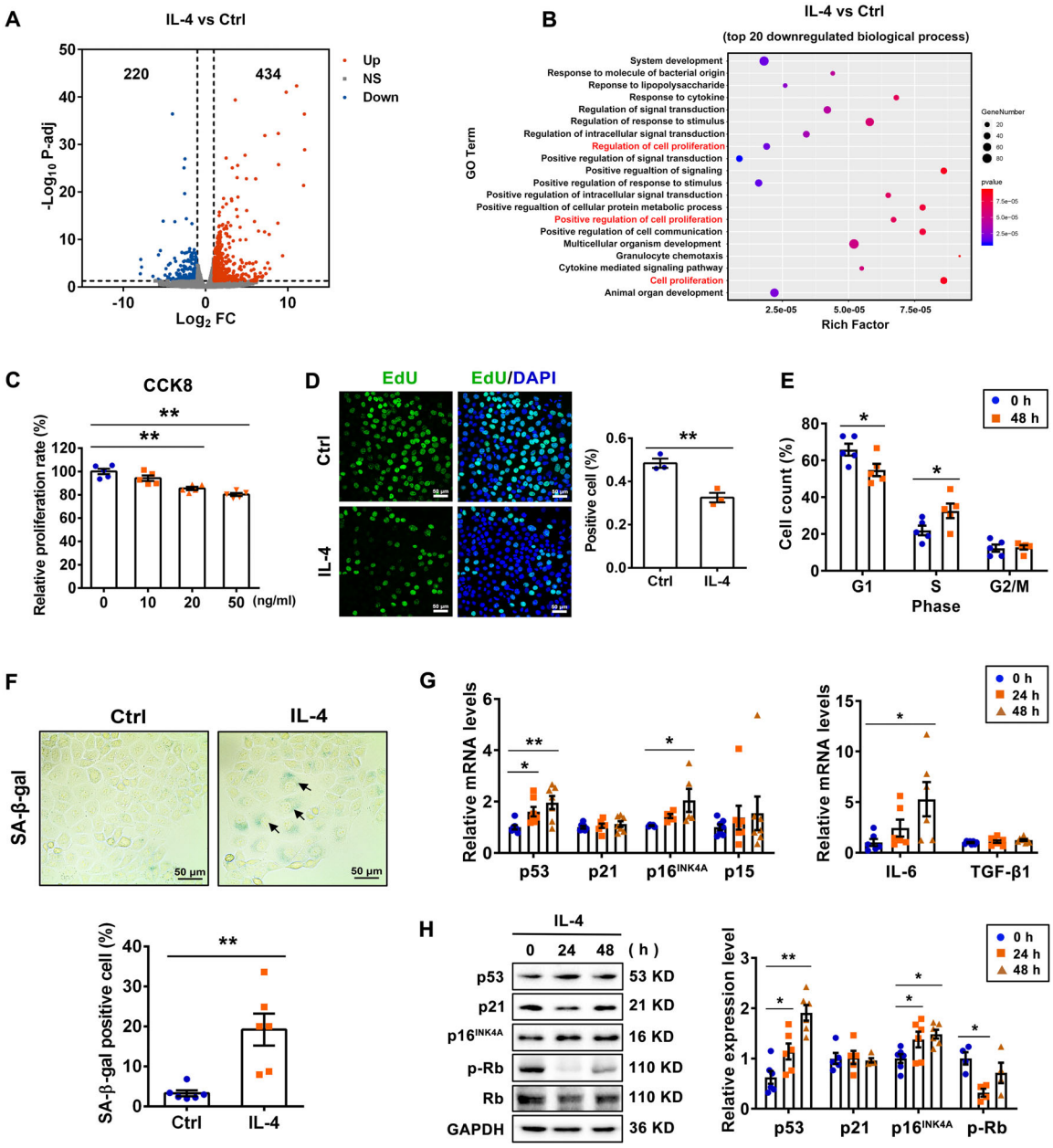

Figure 3. Direct induction of cellular senescence by interleukin-4 (IL-4). **A**, Volcano plot of RNA sequencing in SMG-C6 cells treated with IL-4 (20 ng/ml) for 48 hours (n = 3). Up-regulated genes (ratio of fold change [FC] ≥2) are shown in orange; down-regulated genes (ratio of fold change ≤0.5) are shown in blue. NS = not significant. **B**, The 20 most significantly enriched Gene Ontology (GO) terms for the down-regulated genes. **C**, Changes in proliferative capacity of SMG-C6 cells exposed to different concentrations of IL-4 for 48 hours, quantitated with Cell Counting Kit 8 (CCK8) (n = 5). **D**, Fluorescence images (left) and quantification of positive cells (right) showing changes in proliferative capacity of SMG-C6 cells exposed to IL-4, measured by 5-ethynyl-2′-deoxyuridine (EdU) assay (n = 3). Proliferative nuclei are green; cell nuclei were stained with DAPI. Bars = 50 μm. **E**, Cell cycle analysis for SMG-C6 cells treated with IL-4 (n = 5). **F**, Staining for (top) and quantification of (bottom) senescence-associated (SA) β-galactosidase (β-gal) in SMG-C6 cells treated with IL-4 (n = 6). **Arrows** indicate positive staining. Bars = 50 μm. **G**, Levels of mRNA for p53, p21, p16^{INK4A}, p15, IL-6, and transforming growth factor β1 (TGFβ1) in SMG-C6 cells treated with IL-4 (n = 5–8). **H**, Western blot (left) and quantification (right) of p53, p21, p16^{INK4A}, p-retinoblastoma (p-Rb), and Rb protein expression in SMG-C6 cells (n = 4–6). In **C**–**H**, symbols represent individual samples; bars show the mean ± SEM. * = $P < 0.05$; ** = $P < 0.01$. Color figure can be viewed in the online issue, which is available at http://onlinelibrary.wiley.com/doi/10.1002/art.42052/abstract.

IL-4 had no effect on LDH activity, the proportion of apoptotic cells, or the ratio of Bax to Bcl-2 proteins (Supplementary Figures 7A–C, available on the *Arthritis & Rheumatology* website at http://onlinelibrary.wiley.com/doi/10.1002/art.42052). The senescence markers p53/p21 and p16^{INK4A} are the 2 major mediators that modulate the cell cycle by inhibiting the activity of CDK, which phosphorylates and inactivates the retinoblastoma (Rb) protein. There was an

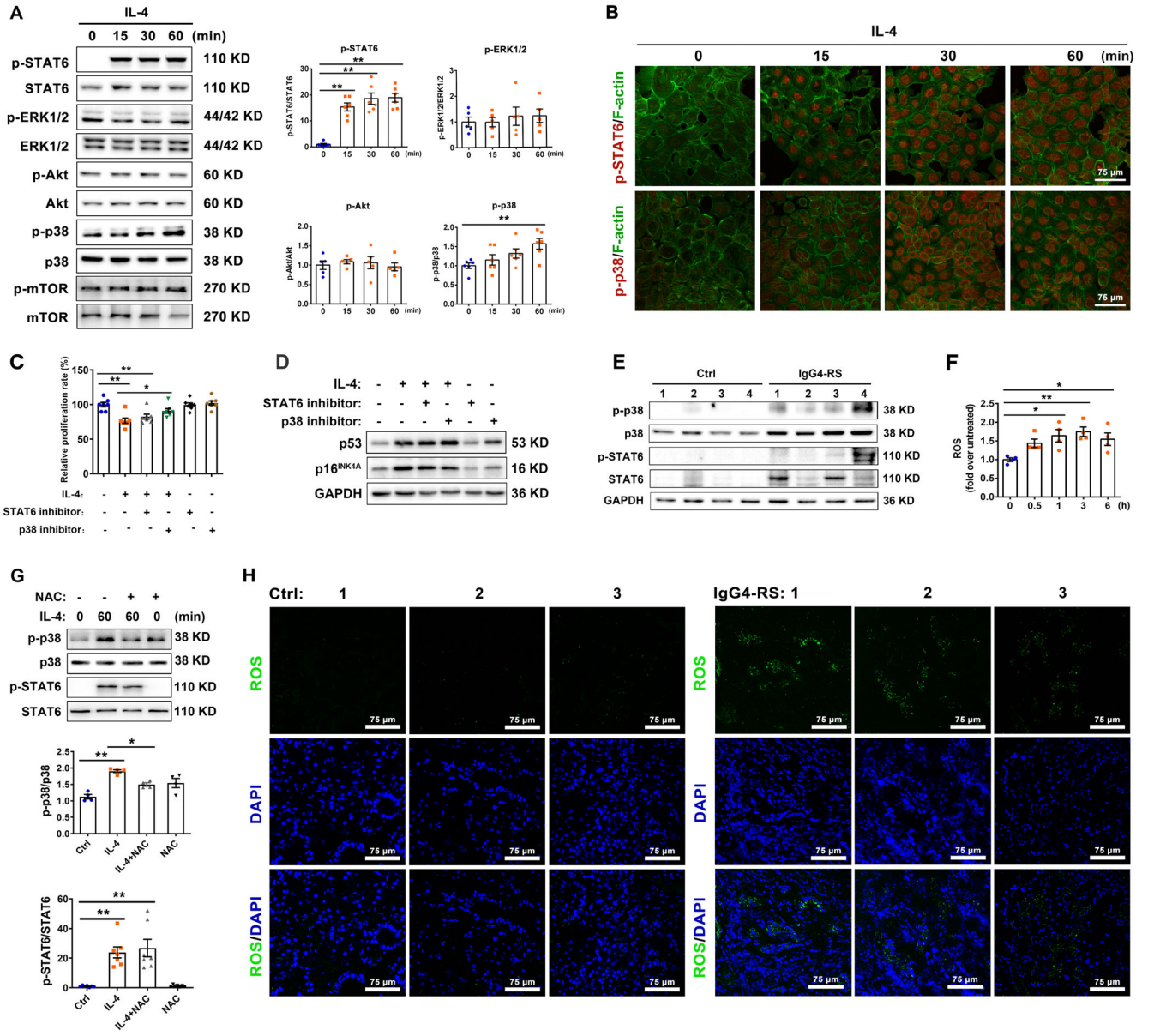

Figure 4. Mediation of interleukin-4 (IL-4)–induced cellular senescence by reactive oxygen species (ROS)/p38 MAPK (p38). **A**, Western blot (left) and quantification (right) of changes in the phosphorylation of STAT6, ERK1/2, protein kinase B (Akt), p38, and mechanistic target of rapamycin (mTOR) after treatment with IL-4 (20 ng/ml) for the indicated time periods (n = 3–6). **B**, Immunostaining for p-STAT6 and p-p38 in SMG-C6 cells stimulated with IL-4. F-actin was stained to show cell outlines. Bars = 75 μm. **C** and **D**, Changes in the proliferative capacity of SMG-C6 cells (**C**) and p53 and p16^{INK4A} protein expression (**D**) in SMG-C6 cells left untreated or pretreated with the STAT6 inhibitor AS1517499 or the p38 MAPK inhibitor SB203580, before IL-4 treatment (n = 7). **E**, Phosphorylation of p38 and STAT6 in submandibular glands (SMGs) from controls and patients with IgG4-related sialadenitis (IgG4-RS). **F**, Changes in intracellular ROS levels in SMG-C6 cells treated with IL-4 for the indicated time periods, determined by flow cytometry (n = 5). **G**, Western blot (top) and quantification (bottom) of the phosphorylation of p38 and STAT6 in SMG-C6 cells pretreated with *N*-acetyl-L-cysteine (NAC; 5 m*M*) before IL-4 treatment (n = 4–7). **H**, ROS staining in SMGs from controls and IgG4-RS patients. Bars = 75 μm. In **A** and **C**, **F**, and **G**, symbols represent individual samples; bars show the mean ± SEM. * = $P < 0.05$; ** = $P < 0.01$. Color figure can be viewed in the online issue, which is available at http://onlinelibrary.wiley.com/doi/10.1002/art.42052/abstract.

increase in the expression of mRNA for p53 and p16^{INK4A} and the SASP factor IL-6, but not p21 (Figure 3G). Western blotting also confirmed that treatment with IL-4 led to an increase in p53 and p16^{INK4A} expression and a decrease in the phosphorylation levels of Rb (Figure 3H). In contrast, stimulation with IFNγ, a characteristic cytokine secreted by Th1 lymphocytes, caused a reduction in the expression of p53 and p21 mRNA (Supplementary Figure 7D). These results suggest that IL-4 could directly induce senescence and lead to growth inhibition in SMG-C6 cells.

Mediation of IL-4–induced cellular senescence by the ROS/p38 MAPK pathway. There are at least 2 distinct signaling pathways triggered by IL-4 that involve STAT6 and the insulin receptor substrate 1/2 (29,30). To investigate the mechanism underlying IL-4–induced cellular senescence, we next examined potential intracellular kinases, including STAT6, ERK1/2, and protein kinase B (Akt), and the potential signals that are thought to induce cellular senescence according to recent studies, such as p38 MAPK and mechanistic target of rapamycin (mTOR) (31). IL-4 stimulation caused up-regulation of p-STAT6, whereas the levels of p-ERK1/2 or p-Akt were unaffected (Figure 4A). Moreover, treatment with IL-4 led to a significant increase in the levels of p-p38 MAPK, but not p-mTOR (Figure 4A and Supplementary Figure 8A, available on the *Arthritis & Rheumatology* website at http://onlinelibrary.wiley.com/doi/10.1002/art.42052). Immunofluorescence staining further showed an increase in the intranuclear expression of both p-STAT6 and p-p38 MAPK after stimulation with IL-4 (Figure 4B). Preincubation with the p38

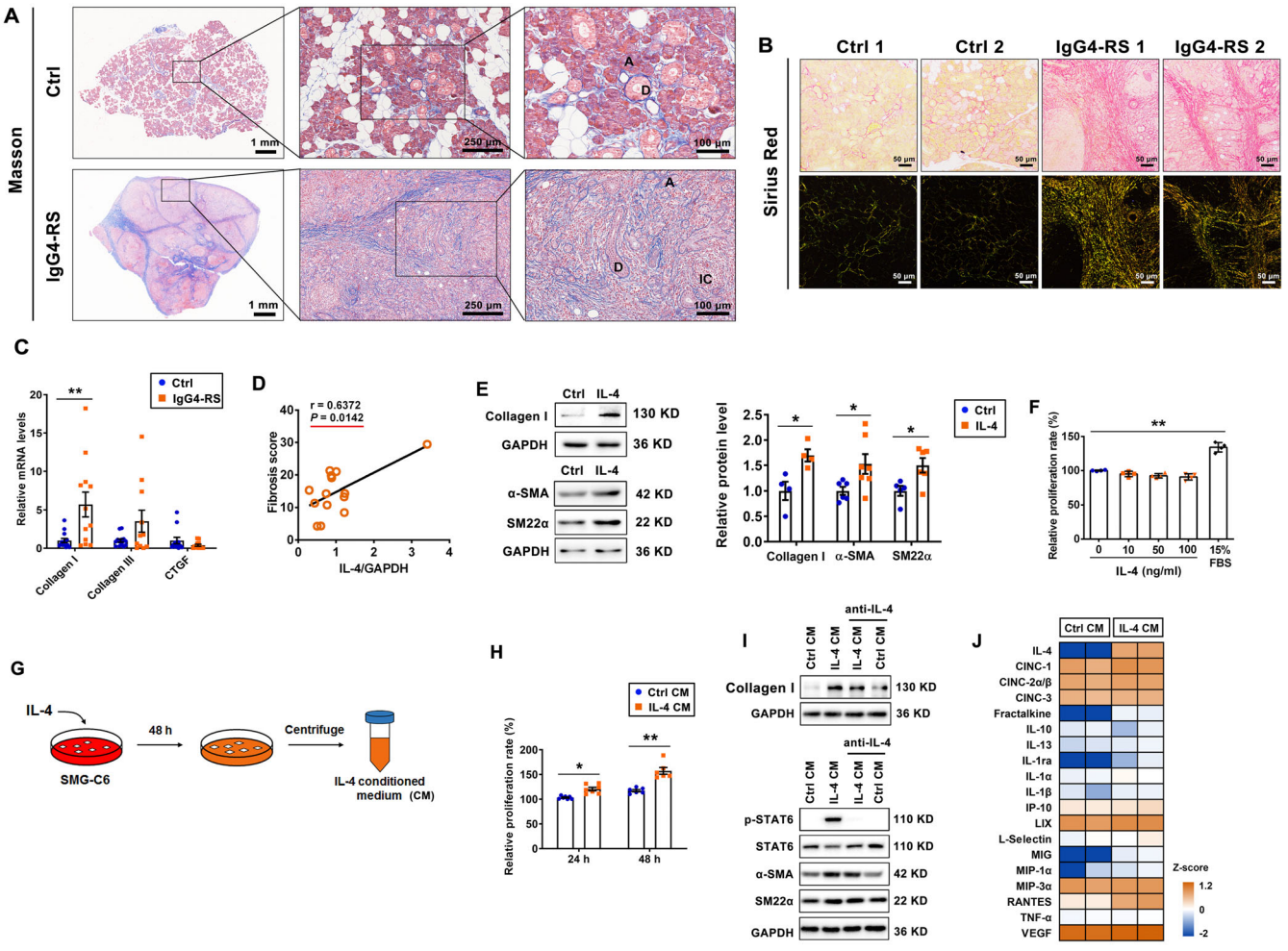

Figure 5. Promotion of fibrosis by interleukin-4 (IL-4)–induced epithelial cell senescence. **A**, Masson's trichrome staining of submandibular gland (SMG) samples from a control and a patient with IgG4-related sialadenitis (IgG4-RS). Middle panels (bars = 250 μm) show higher-magnification views of the boxed areas in the left panels (bars = 1 mm); right panels (bars = 100 μm) show higher-magnification views of the boxed areas in the middle panels. **A** = acini; **D** = ductal cells; **IC** = inflammatory cells. **B**, Light microscopy (top) and polarized microscopy (bottom) images of sirius red staining in SMG samples from controls and IgG4-RS patients. Bars = 50 μm. **C**, Levels of mRNA for type I collagen, type III collagen, and connective tissue growth factor (CTGF) in controls (n = 12–14) and IgG4-RS patients (n = 11–12). **D**, Correlation between IL-4 mRNA level and fibrosis score in SMGs from IgG4-RS patients (n = 14). **E**, Western blot (left) and quantification (right) of type I collagen, α-smooth muscle actin (α-SMA), and SM22α protein expression in rat fibroblasts after IL-4 stimulation (n = 4–7). **F**, Proliferative capacity of rat fibroblasts treated with IL-4 (n = 4). FBS = fetal bovine serum. **G**, Illustration of the procedure for collecting IL-4 conditioned medium. **H**, Proliferative capacity of rat fibroblasts treated with control or IL-4 conditioned medium, measured by Cell Counting Kit 8 (n = 6). **I**, Type I collagen, p-STAT6, α-SMA, and SM22α protein expression in rat fibroblasts incubated in control or IL-4 conditioned medium with or without IL-4 neutralizing antibody (n = 7–8). **J**, Relative expression of cytokines in control and IL-4 conditioned medium. In **C**, **E**, **F**, and **H**, symbols represent individual samples; bars show the mean ± SEM. * = $P < 0.05$, ** = $P < 0.01$. CINC-1 = cytokine-induced neutrophil chemoattractant 1; IL-1Ra = IL-1 receptor antagonist; IP-10 = interferon-γ–inducible 10-kd protein; LIX = lipopolysaccharide-induced CXC chemokine; MIG = monokine induced by interferon-γ; MIP-1α = macrophage inflammatory protein 1α; TNF = tumor necrosis factor; VEGF = vascular endothelial growth factor. Color figure can be viewed in the online issue, which is available at http://onlinelibrary.wiley.com/doi/10.1002/art.42052/abstract.

MAPK inhibitor, SB203580, but not the STAT6 inhibitor, AS1517499, abolished IL-4–induced growth inhibition as well as $p16^{INK4A}$ protein up-regulation (Figure 4C and D). However, the IL-4–induced up-regulation of p53 was unchanged. Consistent with the in vitro studies, there was a significant increase in total and p-p38 MAPK levels, but not STAT6 levels, in SMG lesions from IgG4-RS patients (Figure 4E). These findings suggest that p38 MAPK is an important mediator of IL-4–induced salivary gland epithelial cell senescence.

Oxidative stresses, such as ROS, are thought to cause many age-related chronic diseases (13). In SMG-C6 cells, IL-4 treatment significantly increased intracellular ROS levels (Figure 4F). Preincubation with *N*-acetyl-L-cysteine, a ROS scavenger, inhibited the IL-4–induced phosphorylation of p38 MAPK, whereas the phosphorylation of STAT6 was unaffected (Figure 4G). To determine if intracellular ROS were involved in the progression of IgG4-RS, we detected the level and localization of ROS and found only a few sporadic ROS-positive foci in the SMGs from controls, whereas excessive accumulation of ROS was observed in the cytoplasm of residual epithelial cells in SMG lesions from IgG4-RS patients (Figure 4H and Supplementary Figure 8B). These results indicate that IL-4 induced cellular senescence through the generation of ROS and by subsequently activating the p38 MAPK signal.

IL-4-induced epithelial cell senescence promotes fibrosis by activating fibroblasts both directly and indirectly. Storiform fibrosis is a characteristic feature of the salivary glands in IgG4-RS patients. We observed dense collagen deposition, which mainly consisted of type I collagen and appeared as yellow/orange birefringence under polarized light microscopy, inside the interlobular areas and around the residual epithelial cells in SMGs from IgG4-RS patients (Figures 5A and B). The expression of mRNA for type I collagen, but not type III collagen or connective tissue growth factor, was significantly higher in SMGs from IgG4-RS patients than in SMGs from controls (Figure 5C). We also observed a positive correlation between IL-4 and fibrosis score (Figure 5D).

To further understand the effect of IL-4 on SMG fibrosis, primary rat SMG fibroblasts were isolated and identified by vimentin staining (Supplementary Figure 8C). Stimulation with IL-4 increased the expression of type I collagen, and the myofibroblast markers α-smooth muscle actin (α-SMA) and smooth muscle 22α (SM22α), but had no effect on the proliferative or migration capacity of SMG fibroblasts (Figures 5E and F and Supplementary Figures 8D and E). Additionally, we investigated whether IL-4–induced senescent cells could influence the characteristics of fibroblasts. We collected supernatants from IL-4–treated SMG-C6 cells as conditioned medium (Figure 5G), and then incubated fibroblasts with IL-4 conditioned medium in the presence or absence of IL-4 neutralizing antibodies to eliminate the effect of exogenous IL-4. Incubation with IL-4 conditioned medium significantly enhanced the proliferation of fibroblasts and increased the expression of type I collagen, p-STAT6, α-SMA, and SM22α (Figures 5H and I and Supplementary Figures 9A–C, available on the *Arthritis & Rheumatology* website at http://onlinelibrary.wiley.com/doi/10.1002/art.42052). However, IL-4 conditioned medium did not affect the migration capacity (Supplementary Figures 10A and B, available on the *Arthritis & Rheumatology* website at http://onlinelibrary.wiley.com/doi/10.1002/art.42052). Moreover, the elimination of IL-4 by neutralizing antibody did not affect the IL-4 conditioned medium–induced up-regulation of type I collagen, α-SMA, and SM22α, whereas IL-4–dependent p-STAT6 activation was abolished (Figure 5I). These data suggest that the senescent epithelial cells that were induced by IL-4 could promote the proliferation and phenotype transition of fibroblasts by secreting SASP factors.

To identify potential inducers in the supernatants of IL-4–induced senescent epithelial cells, a cytokine array was performed in IL-4 conditioned medium. The results showed elevated levels of various inflammatory and profibrotic factors, such as IL-1α and IL-1β, as well as chemokines, such as macrophage inflammatory protein 3α and fractalkine (Figure 5J). These findings indicate that IL-4 is an important driver of fibrogenesis that affects fibroblasts both directly and indirectly via the interaction between senescent epithelial cells and fibroblasts in the SMGs of IgG4-RS patients.

IL-4–induced SMG fibrosis and cellular senescence in a mouse model. To further confirm the role of IL-4 in salivary gland epithelial cell senescence and fibrosis, we established a mouse model by injection of murine IL-4 into SMG tissues at multiple sites (Figure 6A). Administering IL-4 did not cause a significant change in body weight, SMG weight, or stimulated salivary flow rate (Figure 6B). Notably, the IL-4–treated glands showed significant atrophy of acinar and ductal cells and collagen deposition with thickened basement lumen compared with the controls (Figure 6C). Masson's trichrome staining revealed that the exogenous IL-4 led to fibrotic lesions in SMGs (Figure 6D). In addition to the fibrotic markers type I collagen and α-SMA, exogenous IL-4 also promoted the expression of $p16^{INK4A}$, but not that of p53. A p38 MAPK activation signal was detected in the IL-4 injection group (Figure 6E). These in vivo studies provide additional evidence regarding the profibrotic effect of IL-4, which may be closely related to the induction of epithelial cell senescence.

DISCUSSION

Fibrosis is the main pathologic feature of IgG4-RS; however, its pathogenic mechanism is unclear. In the present study, we demonstrated that both acinar and ductal cells in the SMGs of IgG4-RS patients exhibit many phenotypic features of senescence. Elevated IL-4 levels in SMG lesions activated the ROS/p38 MAPK-$p16^{INK4A}$ signaling pathway and led to the accumulation of senescent cells. We further showed that IL-4 induces SMG

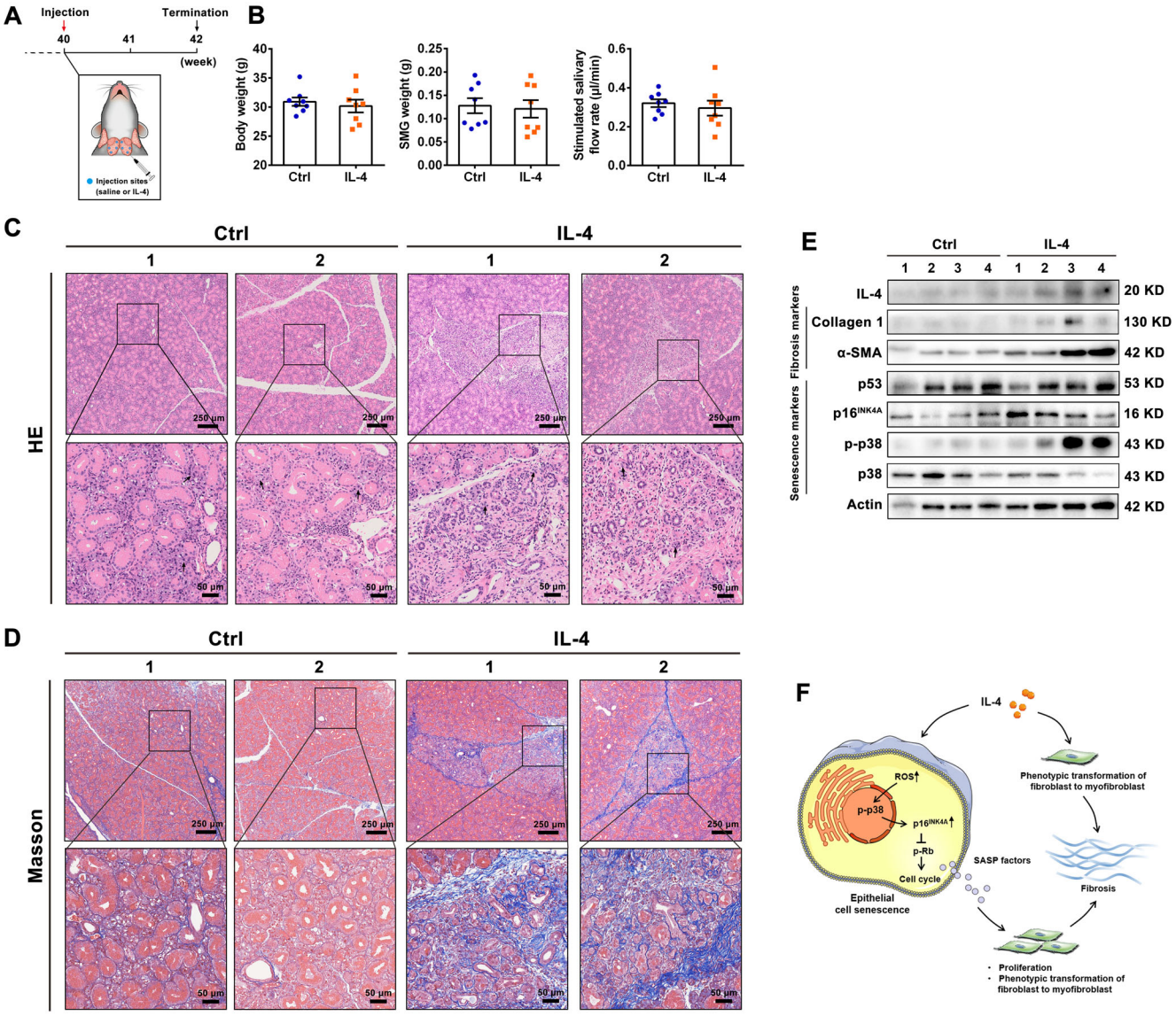

Figure 6. Effects of interleukin-4 (IL-4) on fibrosis and cellular senescence in vivo. **A**, Experimental design of an IL-4–injected mouse model. IL-4 or saline (control) was injected into the submandibular gland (SMG) tissues. **B**, Body weight, SMG weight, and stimulated salivary flow rate in mice injected with saline or IL-4 (n = 8 per group). Symbols indicate individual mice; bars show the mean ± SEM. **C** and **D**, Hematoxylin and eosin (H&E)–stained (**C**) and Masson's trichrome–stained (**D**) sections of SMGs from mice injected with saline or IL-4. Bottom panels (bars = 50 μm) show higher-magnification views of the boxed areas in the top panels (bars = 250 μm). **Arrows** indicate atrophic acini. **E**, Protein expression of the fibrotic markers type I collagen and α-smooth muscle actin (α-SMA), and the senescence markers p53, $p16^{INK4A}$, and p-p38 MAPK (p38), in SMGs from mice injected with saline or IL-4 (n = 4 per group). **F**, Schematic model of the role of IL-4 in the fibrogenesis of IgG4-related sialadenitis (IgG4-RS). The elevation of IL-4 in the SMGs of IgG4-RS patients is an important driver of fibrogenesis through both direct and indirect mechanisms, including 1) production of collagenous proteins by promoting fibroblast differentiation directly, and 2) induction of salivary gland epithelial cell senescence through the reactive oxygen species (ROS)/p38 MAPK-$p16^{INK4A}$ pathway, thereby producing senescence-associated secretory phenotype (SASP) factors to promote fibroblast proliferation and differentiation. p-Rb = p-retinoblastoma. Color figure can be viewed in the online issue, which is available at http://onlinelibrary.wiley.com/doi/10.1002/art.42052/abstract.

fibrosis directly by promoting myofibroblast differentiation and indirectly by inducing senescent epithelial cells that produce SASP factors to activate fibroblasts (Figure 6F).

Storiform fibrosis is a prominent feature of IgG4-RS that leads to the enlargement and dysfunction of salivary glands. Recent studies have demonstrated an accumulation of senescent cells in a number of fibrotic diseases. The lung alveolar epithelium exhibits increased $p16^{INK4A}$ and p21 expression and greater SA β-gal activity in idiopathic pulmonary fibrosis patients and in a mouse model of bleomycin-induced lung injury (32,33). In models of acute kidney injury, G2/M-arrested proximal tubular cell numbers increase and activate c-Jun NH2-terminal kinase signaling, which causes fibrosis by up-regulating profibrotic cytokine production (34). Epidemiologic studies revealed that the incidence

and mortality of fibrotic diseases increases with an aging population, reinforcing the notion that the accumulation of senescent cells might contribute to the onset of organ fibrosis (35,36). However, some studies have shown contrasting results. Senescent hepatic stellate cells reduce the levels of extracellular matrix proteins, enhance the secretion of degrading enzymes, and restrict liver fibrosis (17,37).

To date, it is still unknown whether senescence is present and involved in the fibrosis of IgG4-RS. Through liquid chromatography mass spectrometry/mass spectrometry screening, multiple molecules related to aging were found to be aberrantly expressed in the SMGs of patients with IgG4-RS. In addition, we observed increased lipofuscin accumulation, SA β-gal activity, SASP levels, and enhanced expression of senescence markers (p53 and $p16^{INK4A}$) in IgG4-RS. These findings indicate that salivary acinar and ductal cells undergo senescence during IgG4-RS. Anti-aging compounds or senolytics, which selectively eliminate senescent cells by targeting $p16^{INK4A}$, antiapoptotic proteins, or SASP factors without affecting their normal counterparts, have been shown to efficiently attenuate several age-dependent disorders including fibrosis (14). Although a combination of glucocorticoids and steroid-sparing agents are widely used to treat IgG4-RS, relapses and complications in some patients remain major challenges (38). The present study suggests that targeting cellular senescence might be a potential effective approach for treating IgG4-RS.

The Th2-derived cytokine IL-4 is pleiotropic and may be involved in differentiation, proliferation, or apoptosis depending on the cell type (39,40). A recent study showed that IL-4 induces senescence in human renal carcinoma cell lines by up-regulating p21 through STAT6 and p38 MAPK signals (41). IL-4 serves as a marker of inflammation in cardiac aging, as evidenced by its elevated level in the left ventricle of senescent mice (42). In the present study, we found higher IL-4 expression in local SMG tissues from patients with IgG4-RS, whereas serum IL-4 levels were unchanged, suggesting that IL-4 primarily originates from the infiltrated Th2 lymphocytes and contributes to the local lesions. Moreover, the levels of IL-4 positively correlated with those of $p16^{INK4A}$ and with the degree of fibrosis in IgG4-RS SMG lesions. In vitro, RNA sequencing analysis showed that most of the down-regulated and up-regulated genes were closely related to the regulation of cell proliferation and cell migration, respectively. Since low proliferation is a characteristic of senescent cells, we focused more attention on the down-regulated genes, which indicated that IL-4 might induce senescence in salivary gland epithelial cells.

IL-4 significantly up-regulated SA β-gal activity, changed the morphology of the cells into a senescence phenotype, induced cycle arrest and growth inhibition, caused resistance to apoptosis, and further increased the expression of senescence markers and SASP factors in SMG-C6 cells. In particular, IL-4 induced cellular senescence mainly through $p16^{INK4A}$ and subsequent Rb signal, and not via p53 or p21. The profibrotic role of IL-4 was further proven by the appearance of SMG fibrosis and increased senescence marker expression in mice injected with IL-4, a pathologic phenomenon similar to IgG4-RS. These data demonstrate a causal and direct role of increased IL-4 levels in local lesions in generating salivary gland epithelial cell senescence and fibrosis.

We then explored signal transduction pathways that potentially mediated IL-4–induced epithelial cell senescence. Although STAT6 was significantly activated by IL-4, the inhibition of STAT6 did not affect IL-4–induced senescence. A member of the MAPK family, p38 MAPK mediates numerous cellular processes, such as cellular senescence (31). Partial inactivation of p38 MAPK in p38AF/+ mice, which have mutations in the phosphorylation sites required for activation, led to the attenuation of age-induced up-regulation in the expression of $p16^{INK4A}$, p19, p15, and p21 in multiple tissues. Furthermore, it enhanced the proliferation and regeneration of islets, supporting the notion of an important role of p38 MAPK in the regulation of the cell cycle and senescence (43). In the present study, we found that IL-4 significantly activated p38 MAPK but not ERK1/2, and inhibiting p38 MAPK signaling prevented the IL-4–induced up-regulation of $p16^{INK4A}$ and growth arrest.

We further explored the molecule that linked IL-4 to p38 MAPK. ROS are regarded as the hallmarks of senescence (13). Intracellular ROS generation can serve as a secondary messenger and is responsible for the activation of p38 MAPK in response to cytokines (44). We found that intracellular ROS levels rapidly increased after IL-4 exposure, while treatment with antioxidants abrogated IL-4–induced p38 MAPK activation, suggesting that ROS act as sensors of IL-4 that activate p38 MAPK during the senescence process. In addition, this signaling pathway was detectable in the SMGs from IgG4-RS patients and in the mouse model, thereby supporting the notion of involvement of ROS/p38 MAPK in the development of IgG4-RS.

The transition into SASP makes senescent cells exert beneficial or detrimental effects on the microenvironment by inducing the secretion of cytokines, chemokines, proteases, and growth factors. These SASP factors play important roles in both tissue repair and fibrotic diseases (45). It is well known that fibroblasts are the key effectors that proliferate and differentiate into myofibroblasts in response to injury or inflammation, and lead to the excessive accumulation of extracellular matrix proteins and fibrosis (46). Thus, we investigated both the direct and indirect effects of IL-4 on SMG fibroblasts. IL-4 alone increased collagen synthesis and myofibroblast differentiation but had no effect on proliferation, suggesting that direct IL-4 stimulation only partially activated the fibroblasts. In contrast to this finding, the supernatants collected from IL-4–induced senescent SMG-C6 cells facilitated proliferation, collagen synthesis, and myofibroblast differentiation. Moreover, IL-4 neutralizing antibodies did not eliminate the fibroblast activation induced by IL-4 conditioned medium, which indicated that these effects did not depend on IL-4 but instead on the SASP factors that were secreted by senescent epithelial cells. The secretome of the IL-4–induced senescent cells includes

cytokines and chemokines, which might be important mediators of fibrosis and chronic inflammation in IgG4-RS. The above data show that IL-4 can have a direct and a novel indirect effect, through the interaction between senescent epithelial cells and fibroblasts, in driving the fibrogenesis of IgG4-RS.

In summary, we demonstrate that senescence in salivary epithelial cells is a novel mechanism of fibrogenesis in IgG4-RS. The elevated levels of IL-4 in lesions were responsible for the induction of senescence through the ROS/p38 MAPK-$p16^{INK4A}$ signaling pathway. Moreover, both local IL-4 and the SASP factors derived from IL-4–induced senescent epithelial cells contributed to fibroblast activation, resulting in fibrosis. These findings not only expand our understanding of the pathogenesis of IgG4-RS, but also present a potential intervention strategy for treating IgG4-RS by targeting senescent cells.

ACKNOWLEDGMENT

We thank Professor Guo-He Zhang (National Institute of Dental and Craniofacial Research, NIH, Bethesda, MD) for providing thoughtful suggestions.

AUTHOR CONTRIBUTIONS

All authors were involved in drafting the article or revising it critically for important intellectual content, and all authors approved the final version to be published. Dr. Cong had full access to all of the data in the study and takes responsibility for the integrity of the data and the accuracy of the data analysis.

Study conception and design. Min, Wu, Yu, Cong.
Acquisition of data. Min, Zhu, Mao, Li, Wei, Mei, Cong.
Analysis and interpretation of data. Min, Zhu, Mao, Li, Wei, Mei, Zhang, Wu, Yu, Cong.

REFERENCES

1. Stone JH, Zen Y, Deshpande V. IgG4-related disease. N Engl J Med 2012;366:539–51.
2. Geyer JT, Ferry JA, Harris NL, Stone JH, Zukerberg LR, Lauwers GY, et al. Chronic sclerosing sialadenitis (Küttner tumor) is an IgG4-associated disease. Am J Surg Pathol 2010;34:202–10.
3. Brito-Zerón P, Ramos-Casals M, Bosch X, Stone JH. The clinical spectrum of IgG4-related disease. Autoimmun Rev 2014;13:1203–10.
4. Liu Y, Xue M, Wang Z, Zeng Q, Ren L, Zhang Y, et al. Salivary gland involvement disparities in clinical characteristics of IgG4-related disease: a retrospective study of 428 patients. Rheumatology 2020;59:634–40.
5. Li W, Chen Y, Sun ZP, Cai ZG, Li TT, Zhang L, et al. Clinicopathological characteristics of immunoglobulin G4-related sialadenitis. Arthritis Res Ther 2015;17:186.
6. Inoue D, Yoshida K, Yoneda N, Ozaki K, Matsubara T, Nagai K, et al. IgG4-related disease: dataset of 235 consecutive patients. Medicine (Baltimore) 2015;94:e680.
7. Yamamoto M, Takahashi H, Tanaka H. Differences in clinical features of immunoglobulin G4-related disease between older and younger patients. Geriatr Gerontol Int 2019;19:564–5.
8. Yamamoto M, Takahashi H, Takano K, Shimizu Y, Sakurai N, Suzuki C, et al. Efficacy of abatacept for IgG4-related disease over 8 months. Ann Rheum Dis 2016;75:1576–8.
9. Yamamoto M, Takano K, Kamekura R, Suzuki C, Ichimiya S, Himi T, et al. Stage classification of IgG4-related dacryoadenitis and sialadenitis by the serum cytokine environment. Mod Rheumatol 2018;28:1004–8.
10. Shimatani K, Nakashima Y, Hattori M, Hamazaki Y, Minato N. PD-1^+ memory phenotype $CD4^+$ T cells expressing C/EBPα underlie T cell immunodepression in senescence and leukemia. Proc Natl Acad Sci U S A 2009;106:15807–12.
11. Muñoz-Espín D, Serrano M. Cellular senescence: from physiology to pathology. Nat Rev Mol Cell Biol 2014;15:482–96.
12. Lu L, Guo J, Hua Y, Huang K, Magaye R, Cornell J, et al. Cardiac fibrosis in the ageing heart: contributors and mechanisms. Clin Exp Pharmacol Physiol 2017;44 Suppl:55–63.
13. Hernandez-Segura A, Nehme J, Demaria M. Hallmarks of cellular senescence. Trends Cell Biol 2018;28:436–53.
14. Schafer MJ, Haak AJ, Tschumperlin DJ, LeBrasseur NK. Targeting senescent cells in fibrosis: pathology, paradox, and practical considerations. Curr Rheumatol Rep 2018;20:3.
15. Zhang LM, Zhang J, Zhang Y, Fei C, Wang L, Yi ZW, et al. Interleukin-18 promotes fibroblast senescence in pulmonary fibrosis through down-regulating Klotho expression. Biomed Pharmacother 2019;113:108756.
16. Tominaga K, Suzuki HI. TGF-β signaling in cellular senescence and aging-related pathology. Int J Mol Sci 2019;20:5002.
17. Kong X, Feng D, Wang H, Hong F, Bertola A, Wang FS, et al. Interleukin-22 induces hepatic stellate cell senescence and restricts liver fibrosis in mice. Hepatology 2012;56:1150–9.
18. Marmary Y, Adar R, Gaska S, Wygoda A, Maly A, Cohen J, et al. Radiation-induced loss of salivary gland function is driven by cellular senescence and prevented by IL6 modulation. Cancer Res 2016;76:1170–80.
19. Peng X, Wu Y, Brouwer U, van Vliet T, Wang B, Demaria M, et al. Cellular senescence contributes to radiation-induced hyposalivation by affecting the stem/progenitor cell niche. Cell Death Dis 2020;11:854.
20. Wang X, Bootsma H, Terpstra J, Vissink A, van der Vegt B, Spijkervet FK, et al. Progenitor cell niche senescence reflects pathology of the parotid salivary gland in primary Sjögren's syndrome. Rheumatology (Oxford) 2020;59:3003–13.
21. Pringle S, Wang X, Verstappen GM, Terpstra JH, Zhang CK, He A, et al. Salivary gland stem cells age prematurely in primary Sjögren's syndrome. Arthritis Rheumatol 2019;71:133–42.
22. Kobayashi S, Kamino Y, Hiratsuka K, Kiyama-Kishikawa M, Abiko Y. Age-related changes in IGF-1 expression in submandibular glands of senescence-accelerated mice. J Oral Sci 2004;46:119–25.
23. Kilkenny C, Browne W, Cuthill IC, Emerson M, Altman DG. Animal research: reporting in vivo experiments: the ARRIVE guidelines. Br J Pharmacol 2010;160:1577–9.
24. Umehara H, Okazaki K, Masaki Y, Kawano M, Yamamoto M, Saeki T, et al. Comprehensive diagnostic criteria for IgG4-related disease (IgG4-RD), 2011. Mod Rheumatol 2012;22:21–30.
25. Debacq-Chainiaux F, Erusalimsky JD, Campisi J, Toussaint O. Protocols to detect senescence-associated beta-galactosidase (SA-βgal) activity, a biomarker of senescent cells in culture and *in vivo*. Nat Protoc 2009;4:1798–806.
26. Evangelou K, Gorgoulis VG. Sudan Black B, the specific histochemical stain for lipofuscin: a novel method to detect senescent cells. Methods Mol Biol 2017;1534:111–9.
27. Akiyama M, Suzuki K, Yamaoka K, Yasuoka H, Takeshita M, Kaneko Y, et al. Number of circulating follicular helper 2 T cells correlates with IgG4 and interleukin-4 levels and plasmablast numbers in IgG4-related disease. Arthritis Rheumatol 2015;67:2476–81.
28. Della-Torre E, Bozzalla-Cassione E, Sciorati C, Ruggiero E, Lanzillotta M, Bonfiglio S, et al. A $CD8\alpha^-$ subset of $CD4^+SLAMF7^+$ cytotoxic T cells is expanded in patients with IgG4-related disease

and decreases following glucocorticoid treatment. Arthritis Rheumatol 2018;70:1133–43.

29. Hou J, Schindler U, Henzel WJ, Ho TC, Brasseur M, McKnight SL. An interleukin-4-induced transcription factor: IL-4 Stat. Science 1994; 265:1701–6.
30. Pernis A, Witthuhn B, Keegan AD, Nelms K, Garfein E, Ihle JN, et al. Interleukin 4 signals through two related pathways. Proc Natl Acad Sci U S A 1995;92:7971–5.
31. Xu Y, Li N, Xiang R, Sun P. Emerging roles of the p38 MAPK and PI3K/AKT/mTOR pathways in oncogene-induced senescence. Trends Biochem Sci 2014;39:268–76.
32. Lehmann M, Korfei M, Mutze K, Klee S, Skronska-Wasek W, Alsafadi HN, et al. Senolytic drugs target alveolar epithelial cell function and attenuate experimental lung fibrosis *ex vivo*. Eur Respir J 2017; 50:1602367.
33. Schafer MJ, White TA, Iijima K, Haak AJ, Ligresti G, Atkinson EJ, et al. Cellular senescence mediates fibrotic pulmonary disease. Nat Commun 2017;8:14532.
34. Yang L, Besschetnova TY, Brooks CR, Shah JV, Bonventre JV. Epithelial cell cycle arrest in G2/M mediates kidney fibrosis after injury. Nat Med 2010;16:535–43.
35. Dzeshka MS, Shahid F, Shantsila A, Lip GY. Hypertension and atrial fibrillation: an intimate association of epidemiology, pathophysiology, and outcomes. Am J Hypertens 2017;30:733–55.
36. Ley B, Collard HR. Epidemiology of idiopathic pulmonary fibrosis. Clin Epidemiol 2013;5:483–92.
37. Jin H, Lian N, Zhang F, Chen L, Chen Q, Lu C, et al. Activation of PPARγ/P53 signaling is required for curcumin to induce hepatic stellate cell senescence. Cell Death Dis 2016;7:e2189.
38. Hong X, Zhang YY, Li W, Liu YY, Wang Z, Chen Y, et al. Treatment of immunoglobulin G4-related sialadenitis: outcomes of glucocorticoid therapy combined with steroid-sparing agents. Arthritis Res Ther 2018;20:12.
39. Nelms K, Keegan AD, Zamorano J, Ryan JJ, Paul WE. The IL-4 receptor: signaling mechanisms and biologic functions. Annu Rev Immunol 1999;17:701–38.
40. Horvath CM. STAT proteins and transcriptional responses to extracellular signals. Trends Biochem Sci 2000;25:496–502.
41. Kim HD, Yu SJ, Kim HS, Kim YJ, Choe JM, Park YG, et al. Interleukin-4 induces senescence in human renal carcinoma cell lines through STAT6 and p38 MAPK. J Biol Chem 2013;288: 28743–54.
42. Ma Y, Chiao YA, Clark R, Flynn ER, Yabluchanskiy A, Ghasemi O, et al. Deriving a cardiac ageing signature to reveal MMP-9-dependent inflammatory signalling in senescence. Cardiovasc Res 2015;106: 421–31.
43. Wong ES, Le Guezennec X, Demidov ON, Marshall NT, Wang ST, Krishnamurthy J, et al. p38MAPK controls expression of multiple cell cycle inhibitors and islet proliferation with advancing age. Dev Cell 2009;17:142–9.
44. Tormos AM, Taléns-Visconti R, Nebreda AR, Sastre J. p38 MAPK: a dual role in hepatocyte proliferation through reactive oxygen species. Free Radic Res 2013;47:905–16.
45. Freund A, Orjalo AV, Desprez PY, Campisi J. Inflammatory networks during cellular senescence: causes and consequences. Trends Mol Med 2010;16:238–46.
46. Rockey DC, Bell PD, Hill JA. Fibrosis—a common pathway to organ injury and failure. N Engl J Med 2015;372:1138–49.